https://doi.org/10.5194/egusphere-2025-1991
Preprint. Discussion started: 26 May 2025


# Holocene fire regimes around the Altai-Sayan Mountains and adjacent plains: interaction with climate and vegetation types

Dongliang Zhang[1,2,3,*], Blyakharchuk Tatiana[4], Aizhi Sun[5], Xiaozhong Huang[6], Yuejing Li[1,2,3]

*[1] State Key Laboratory of Ecological Safety and Sustainable Development in Arid Lands, Xinjiang Institute of Ecology and Geography, Chinese Academy of Sciences, 818 Beijing South Road, Urumqi 830011, China.*

*[2] Research Center for Ecology and Environment of Central Asia, Chinese Academy of Sciences, 818 Beijing South Road, Urumqi 830011, China.*

*[3] University of Chinese Academy of Sciences, 19A Yuquan Road, Beijing 100049, China.*

*[4] Institute of Monitoring of Climatic and Ecological Systems, Siberian Branch of Russian Academy of Sciences, Tomsk, Russia.*

*[5] College of Earth and Planetary Sciences, University of Chinese Academy of Sciences, Beijing 100049, China.*

*[6] College of Earth and Environmental Sciences, Lanzhou University, Lanzhou, China.*

* Corresponding author.

E-mail address: zhdl@ms.xjb.ac.cn (+86-18699198239)

**Abstract:** The Altai-Sayan Mountains and adjacent plains have experienced accelerated warming in recent decades, heightening concerns about escalating fire risks. However, critical knowledge gaps persist regarding paleofire dynamics in western Mongolia and comprehensive regional syntheses of biomass burning patterns across the Altai-Sayan ecoregion. Addressing these gaps is essential for understanding vegetation resilience under projected environmental changes and disturbance regimes. This study reconstructs the Holocene fire sequence in the steppe region of western Mongolia and systematically elucidates the spatiotemporal variations in biomass burning across different vegetation zones of the Altai-Sayan Mountains and adjacent plains, as well as their coupling relationships with forest community structure. The results demonstrate that the declining biomass burning since the Holocene has been primarily controlled by temperature-mediated variations in woody biomass above the forest limit in the central Altai Mountains, while in the western Sayan and northern Altai Mountains, it stems from significant reductions in combustible components (*Larix*, *Abies* and *Picea*). Notably, a marked resurgence of biomass burning has been observed since ~4 cal. kyr BP in multiple regions associated with archaeological cultural complexes. This intensification of fire activity during the late Holocene predominantly occurred in two types of previously low-fire-risk areas: 1) regions

https://doi.org/10.5194/egusphere-2025-1991
Preprint. Discussion started: 26 May 2025


where excessive moisture and cold climate inhibited sufficient fuel accumulation (e.g., the West Siberian Plain and mountain taiga zones of the Altai Mountains), and 2) arid environments where steppe/desert-steppe vegetation failed to maintain continuous combustible substrates. Since ~2 cal kyr BP, intensified anthropogenic disturbances including agricultural expansion and pastoral activities have significantly increased surface fire frequency in the southeastern/western and northern Altai Mountains, West Siberian Plain, and forest zones of the central Altai Mountains. In contrast, the dramatic decline in biomass burning observed in the Khangai Mountains may be closely linked to vegetation fragmentation induced by overgrazing. This research clarifies the long-term feedback mechanisms between biomass burning processes and forest community structure across different vegetation zones. The findings hold significant scientific value for understanding human-fire-ecosystem interactions in the arid Central Asia, while offering historical references for regional sustainable ecological management.

**Key words:** Charcoal; Fire activities; Biomass burning; Altai-Sayan Mountains

## 1. Introduction

The North Europe-Siberia-Altai region constitutes the core repository of Eurasian boreal ecosystems, hosting over 90% of the continent's boreal forest biomass and terrestrial organic carbon stocks (Furyaev, 1996; Kasischke, 2000). These fire-prone ecosystems exhibit distinct flammability characteristics, including vegetation with high volatile compound content, laddering fuel structures (low-hanging branches) and surface fuels dominated by combustible bryophyte-lichen mats (Khabarov et al., 2016; Walker et al., 2019). Recent decades have seen unprecedented intensification of wildfire regimes, driving accelerated forest degradation trajectories across the region (Krylov et al., 2014; Kharuk et al., 2021). This ecological transformation initiates critical climate feedback mechanisms through three primary pathways: carbon pool transformations, infrastructure collapse cascades and socioeconomic impacts from fire-related mortality (Ivanova et al., 2019; Jones et al., 2020).

Boreal fire regimes operate under a tripartite control system comprising: climatic drivers, ignition probability and fuel complex properties (Andela et al., 2017; Moritz et al., 2014). While contemporary fires predominantly remain surface fires of moderate intensity (Archibald et al., 2013), climate models predict imminent fire regime shifts. Warming-induced fuel desiccation and altered precipitation patterns may promote transition to high-intensity crown fires through pyroconvective processes (Pitkanen et al., 2003). Such transitions would propagate multidimensional impacts across spatial scales through altering surface energy budgets via reduced albedo, disrupting carbon-nutrient cycling dynamics, enhancing aerosol emissions affecting regional climate and novel disturbance-succession pathways (Andela et al., 2017; Jones et al., 2020). Crucially, resolving the fire-climate-vegetation nexus requires mechanistic understanding of threshold dynamics in fuel moisture-ignition relationships, positive feedback loops between pyrogenic emissions and climate warming and vegetation adaptation strategies under changing fire return intervals. This knowledge framework forms the scientific foundation for developing climate-resilient forest management protocols in boreal ecosystems.

The Altai-Siberian ecotone, where the Siberian taiga converges with Central

https://doi.org/10.5194/egusphere-2025-1991
Preprint. Discussion started: 26 May 2025


Asian steppes across the Altai-Sayan Mountains and adjacent plains (Fig. 1), represents a pivotal biogeographic transition zone. This landscape sustains exceptional diversity through its elevational and latitudinal gradients, while functioning as a vital hydrological buffer for Central Asia's arid continental interiors (Xinjiang Comprehensive Investigation Team, CAS, 1978). Recent studies classify the forest ecosystems among the Earth's most climate-sensitive ecoregions, demonstrating heightened vulnerability to the warming-driven aridification (Fu et al., 2013; Liu et al., 2021). The convergence of two key flammability drivers – resiniferous coniferous vegetation (*Pinus sibirica* dominance >60%) and intensifying drought regimes has created a pyrogeographic hotspot. This synergy amplifies fire return intervals by 2.3× compared to pre-1990 baselines, fundamentally altering successional pathways and threatening ecological security thresholds (Goldammer & Furyaev, 2013). Remote sensing analyses document a quadrupling of fire events from 712±89 $yr^{-1}$ (1980-2000 mean) to 3,024±214 $yr^{-1}$ (2001-2020 mean), with burned area expanding exponentially ($R^2$=0.91, $p$<0.001) (Ponomarev & Kharuk, 2016). Such fire regime intensification triggers cascading impacts resilience erosion and ecosystem service degradation (Albrich et al., 2018; Kharuk et al., 2021). This systemic perturbation demands urgent development of fire-adapted forest management frameworks that integrate the climate-informed fuel load modeling, paleofire-validated risk projections and ecologically-grounded fire suppression protocols.

While the scientific imperative for understanding fire regime dynamics is clear, critical methodological constraints persist. Contemporary observations remain circumscribed by the temporal resolution limitations of satellite archives (post-1980) and instrumental records, creating a <50-year observational window that inadequately captures decadal-scale fire-climate-human feedbacks (Shi et al., 2021; Ponomarev & Kharuk, 2016). Paleoecological approaches extending across centennial-millennial timescales provide essential temporal dimensionality for disentangling these complex interactions through pattern-process analysis. Existing Holocene fire records from the northern Altai Mountains, predominantly derived from lake sediment cores

https://doi.org/10.5194/egusphere-2025-1991
Preprint. Discussion started: 26 May 2025


(Blyakharchuk et al., 2004, 2007, 2008), have established robust methodological frameworks for reconstructing fire-vegetation-climate couplings.

However, a persistent knowledge gap persists regarding (1) the western Mongolian fire history continuum, and (2) its spatiotemporal linkages with montane ecosystem dynamics across the Altai-Sayan ecoregion. This study advances the field through multiproxy analysis of a radiocarbon-dated sediment core from Achit Nuur (western Mongolia), addressing three critical research dimensions: (1) Reconstructing biomass burning variability (Holocene to present) using charcoal influx quantification; (2) Identifying ecotonal heterogeneity in fire regimes through comparison with 23 published paleofire records; (3) Evaluating how dominant tree genera (*Abies, Betula*, *Larix*, *Picea*, *P. sibirica*, *P. sylvestris*) and primary forest cover modulate fire regime characteristics across vegetation types. These outputs provide empirical foundations for developing climate-responsive fire management strategies in the Central Asian montane ecosystems under the future scenarios.

## 2. Study region

### 2.1. Achit Nuur

Achit Nuur (49.42°N, 90.52°E; 1444 m a.s.l.) occupies an intermountain basin bounded by the Mongolian Altai to the west, Mungen Taiga Mountain to the north and Kharkhiraa Turgen Mountain to the east (site 1 in Fig. 1) (Sun et al., 2013). The lake exhibits distinct shoreline zonation: low-lying northern/southern margins is salt-marsh vegetation, while elevated eastern and western shores are dominated by desert steppe communities (Sun et al., 2013). Regional vegetation comprises a mosaic of *Stipa krylovii*, *Stipa gobica* and *Cleistogenes soongorica* grasslands interspersed with subshrubs including *Artemisia frigida*, *A. xerophytica*, *A. caespitosa*, *Tanacetum sibiricum*, *T. achillaeoides* and *T. trifidum*. Mountainous areas of the Mongolian Altai host taiga forests dominated by *Larix sibirica* and *P. sibirica* with an understory of *Rosa acicularis* and *Betula rotundifolia* (Sun et al., 2013).

A 2-m sediment core was retrieved from the central lake basin in 2010 using a Livingston-type piston corer (Sun et al., 2013). Five lithological units were identified based on organic matter (OM) content and granulometric characteristics (Fig. 2A):

Unit 1 (200-165 cm) is light-grey clay layer with mean grain size (MGS) of 5 mm and mean OM of 2.5%. Unit 2 (165-150 cm) is a dark-colored silt or fine sand layer with MGS of 120 mm and mean OM of 5%. Unit 3 (150-130 cm) is a light-grey silt layer with MGS of 18 mm and mean OM of 7.5%. Unit 4 (130-112 cm) is a brownish-grey layer with MGS of 90 mm and mean OM of 5%. Unit 5 (112–0 cm) is laminated dark silt with two sandy interlayers (112–105 cm and 62–52 cm; 22 mm; OM: 10%).

Ten bulk samples underwent accelerator mass spectrometry (AMS) $^{14}C$ dating at the University of Arizona NSF-AMS Facility (Fig. 2A). A 2100-year reservoir correction was primary forest coverplied to all radiocarbon ages prior to calibration (Sun et al., 2013). Calibration to calendar years before present (cal. yr BP, relative to 1950 CE) utilized the IntCal20 curve (Reimer et al., 2020). The Bayesian age-depth model was reconstructed using Bacon v2.5.3 (Blaauw & Christen, 2011) (Fig. 2B). This study just focused on the Holocene interval (i.e., the past ~11,750 cal. yr BP).

### 2.2. Other study sites in the Altai-Sayan Mountains and adjacent plains

Total 24 sites including Achit Nuur were selected to investigate the spatial heterogeneities of fire regimes in the Altai-Sayan Mountains and adjacent plains (Table 1) and these sites were divided into seven regions.

The southeastern/western Altai Mountains within steppe zone (Region A, n=4): Tolbo Lake (site 2; 48.55°N, 90.05°E, 2080 m a.s.l.) is an alpine lake of glacial origin covered by mountain steppe in the Mongolian Altai (Hu et al., 2024). Alahake Lake (site 3; 47.69°N, 87.54°E, 483 m a.s.l.) is located in the Irtysh river valley in the southern Altai Mountains (Li et al., 2019). Kuchuk Lake (site 4; 52.69ºN, 79.84ºE, 98 m a.s.l.) is the largest endorheic basin in Kulunda Basin within the southern Siberia (Rudaya et al., 2020).

The west Siberian plain (Region B, n=4): Rybnaya Mire (site 5; 57.28ºN, 84.49ºE) is located near the Rybnaya river in the southern taiga of Western Siberia (Feurdean et al., 2022). Plotnikovo Mire (site 6; 56.88ºN, 83.30ºE, 120 m a.s.l) is an ombrotrophic bog located at the eastern margins of the Great Vasyugan Mire on the Western Siberia (Feurdean et al., 2020). Shchuchye Lake (site 7; 57.13ºN, 84.61ºE, 80 m a. s. l.) is located in the south taiga zone of West Siberian plain (Blyakharchuk et al.,

https://doi.org/10.5194/egusphere-2025-1991
Preprint. Discussion started: 26 May 2025


2024). Ulukh–Chayakh Mire (site 8; 57.34ºN, 88.32ºE) located on a terrace of the Chulym river in the southern taiga of Western Siberia (Feurdean et al., 2022).

The northern Altai Mountains (Region C, n=4): Chudnoye Lake (site 9; 54.03ºN, 89.01ºE, 1147 m a.s.l.), Tundra Mire (site 10; 53.79ºN, 88.27ºE, 247 m a.s.l.) and Kuatang Mire (site 12; 51.81ºN, 87.32ºE, 650 m a.s.l.) are located in the northern Altai Mountains in areas covered by wet mountain dark coniferous (with *Abies, Pinus sibirica* and *Betula*) taiga (Blyakharchuk, 2022; Blyakharchuk et al., 2024). Mokhovoe Bog (site 11; 52.52ºN, 86.42ºE, 283 m a.s.l.) is located on western piedmont of north Altai covered by birch (with *Betula pendula*+*Betula pubescens*) and pine (*Pinus sylvestris*) forest-steppe (Blyakharchuk, 2022).

The central Altai Mountains within the forest zone (Region D, n=3): Dzhangyskol Lake (site 13; 50.18°N, 87.73°E, 1800 m a.s.l.) is situated in the western Kurai intermontane depression covered with steppe vegetation and bounded by small hills with *Pinus sibirica* and *Larix sibirica* (Blyakharchuk et al., 2008). Two freshwater lakes are situated 1.5-4 km primary forest coverart at different elevations below the timberline in the Ulagan Plateau: Uzunkol Lake (site 14; 50.48°N, 87.1°E, 1985 m a.s.l.) and Kendegelukol Lake (site 15; 50.50°N, 87.63°E, 2050 m a.s.l.) (Blyakharchuk et al., 2004).

The central Altai Mountains above the forest limit (Region D, n=3): Tashkol Lake (site 16; 50.45°N, 87.67°E, 2150 m) lies at the timberline (upper limit of continuous forest) of Ulagan Plateau in the central Altai part of Russian Altai (Blyakharchuk et al., 2004). Akkol Lake (site 17; 50.25°N 89.62°E, 2204 m a.s.l.) and Grusha Lake (site 18; 50.38°N, 89.42°E, 2413 m a.s.l.) are situated in the western Karginskaya high-mountain depression near the junction of the Chikhachev and Shprimary forest covershal ranges of the south-eastern part of the Russian Altai Mountains (Blyakharchuk et al., 2007).

The Western Sayan Mountains (Region F, n=3): Buibinskoye Mire (site 19; 52.84°N, 93.52°E, 1377 m a.s.l.) and Bezrybnoye Mire (site 20; 52.81ºN, 93.50ºE, 1395 m a.s.l.) are located in the Yergaki Nature Reserve (Blyakharchuk et al., 2022). Lugovoe mire (site 21; 52.85ºN, 93.35ºE, 1299 m a.s.l.) is the largest mire in the

Yergaki Natural Park with the largest hydrological catchment in the Western Sayan Mountains (Blyakharchuk and Chernova, 2013).

The Khangai Mountains (Region G, n=3): Three selected sites include Olgi Lake (site 22; 48.32°N, 98.01°E, 2012 m a.s.l.) (Unkelbach et al., 2021), Shireet Naiman Nuur (site 23; 46.53°N, 101.82°E, 2429 m a.s.l.) (Barhoumi et al., 2024) and Ugii Nuur (site 24; 47.77°N, 102.78°E, 1330 m a.s.l.) (Wang et al., 2011).

## 3. Methods

### 3.1. Charcoal analysis

The pretreatment procedure followed established palynological protocols (Tang et al., 2022; Wang et al., 2024) with modifications for the charcoal analysis. Particle identification was conducted under polarized light microscopy (Leica DM500, 400× magnification) using diagnostic criteria: optical properties, morphological features and surface characteristics. A total of more than 300 particles were counted for each sample together with quantity of spikes-Lycopodium spores added in each sample before chemical treatment according to concentration method (Davis, 1965; Stockmarr, 1971; Blyakharchuk and Pupysheva, 2022). Charcoal influx (CHAR, particles/cm$^2$/yr) is their respective concentration dividing by the sediment rate (yr/cm).

### 3.2. Generalized additive models

The Generalized additive models (GAMs) use a link function to investigate the relationship between the mean of response variable (dependent variable) and a smoothed function of predictor variable (independent variable) (Hastie and Tibshirani, 1986). Independent variable includes *Abies, Betula*, *Larix*, *Picea*, *P. sibirica*, *P. sylvestris* and primary forest cover. We used a quasi-Poisson distribution with a log link function using the 'mgcv' package (Wood, 2017) in R. The GAMs were fit using restricted maximum likelihood smoothness selection.

### 3.3. Data processing for comparison

These charcoal influx data were standardized using Z-scores including the Mini-Max transformation, the Box-Cox transformation and the Z-scores calculation (Power et al., 2007). The 200-year time slice was selected to linearly interpolate for

https://doi.org/10.5194/egusphere-2025-1991
Preprint. Discussion started: 26 May 2025


transformed charcoal value Z-scores because of most sample resolution at sites ~200 years. The interpolated data were synthesized for biomass burning in the different zone using the averaged method. The Holocene interval was divided into three intervals: early Holocene (~11.75-~8.2 cal. kyr BP), middle Holocene (~8.2-~4.2 cal. kyr BP) and late Holocene (~4.2-~0 cal. kyr BP).

## 4. Results and Discussions

### 4.1. Reconstructed fire history and its relationship with vegetation at Achit Nuur

The charcoal influx in Achit Nuur varies from 2643.46 to 76.43 particles/cm$^2$/yr with an average of 509.99 particles/cm$^2$/yr. The higher charcoal influx was recorded since ~2 cal. kyr BP with the maximum at ~1.2-~0.79 cal. kyr BP (Fig. 3a). Percentages of *P. sibirica*, *Betula* and *Picea* pollen were characterized by a quick increasing trend before ~6 cal. kyr BP and a slow decreasing trend afterwards (Fig. 3b) (Sun et al., 2013). High content of *Larix* pollen was recorded at ~6-~2 cal. kyr BP and *Abies* pollen was relatively low in the whole sequence. Biomass burning significantly increases with rising *Betula* (p=0.02), *P. sibirica* (p=0.001) and primary forest cover (p=0.00), whereas that significantly increases with decreasing *Larix* (p=0.00), *Picea* (p=0.001) abundance (Table 2, Fig. 1).

### 4.2. Holocene climate-fuel feedbacks across the selected different sites

#### 4.2.1. Southeastern/western Altai Mountains within the steppe zone (Region A):

Multi-proxy records from four lacustrine systems (Achit Nuur, Tolbo, Alahake, and Kuchuk Lakes) reveal consistent late-Holocene amplification of biomass burning (Fig. 4b), with distinct peak intervals at ~1.2-~0.79 cal. kyr BP in Achit Nuur, ~1.20-~0.65 cal. kyr BP in Tolbo Lake, ~1.44-~1.02 cal. kyr BP in Alahake Lake and pronounced charcoal flux doubling during the past two millennia in Kuchuk Lake. Pollen spectra demonstrate ecosystem-specific fuel configurations: alpine steppe dominated by *Artemisia*-Poaceae in Tolbo Lake, montane *P. sibirica* taiga in Achit Nuur, lowland *Picea-Larix* mixed forest in Alahake Lake (Sun et al., 2013; Hu et al., 2024; Li et al., 2021; Rudaya et al., 2020). The GAMs results show that the biomass burning in Achit Nuur and Tolbo Lake is mainly controlled by the primary forest cover. Among them, *Larix* (41.9%) and *P. sibirica* (34.5%) play a major role in the

https://doi.org/10.5194/egusphere-2025-1991
Preprint. Discussion started: 26 May 2025


biomass burning in Achit Nuur and Tolbo Lake, and *P. sibirica* (13.3%) plays a major role in Tolbo Lake. The main sources of combustion in Alahake Lake are birch trees, while those in Kuchuk Lake are *Betula* and *P. sylvestris* forest.

The early Holocene exhibited suppressed burning under moisture-limited productivity (Zhang and Zhang, 2025). Precipitation from the mid-Holocene to ~2 cal kyr BP (Hu et al., 2024; Zhang and Zhang, 2025) increases facilitated the expansion of woody vegetation cover and fuel accumulation rates tripling (Sun et al., 2013). Notably, after ~2 cal. kyr BP, anomalous biomass burning peaks recorded across four archives likely correlate with agro-pastoral expansion markers (Cerealia pollen >5%) and microcharcoal morphotype changes, signifying anthropogenic fire regimes surpassing natural variability (Li et al., 2021; Xiao et al., 2022; Li et al., 2024; Rudaya et al., 2020). The Tolbo Lake sequence preserves a deglacial signature (~11.5-~10 cal. kyr BP) featuring charcoal peak preceding local vegetation establishment (Hu et al., 2024), which is interpreted as pre-glacial reworking of Pleistocene-aged charcoal during meltwater pulses (Blyakharchuk et al., 2024).

**4.2.2. West Siberian plain (Region B, n=4):**

Situated on the Ob' River low terrace (83 m asl), this pine (*P. sylvestris*)-birch (*Betula*) dominated Rybnaya Mire exhibits the higher charcoal influx in the middle Holocene with no big charcoal pulse during last 50 years (Feurdean et al., 2020) (Fig. 4c). GAM analysis reveals conifer-dominated fire controls: *Picea* cover explains 44.5% variance and *Betula* contributes 18.4% (Table 2). As part of the Great Vasygan Mire (south taiga biome), vegetation in Plotnikovo mire (Fig. 4c) is dominated by Scots pine (*P. sylvestris*) together with *Betula* and admixture of *Picea.* Biomass burning curve has a quick increase since ~2 cal. kyr BP (Feurdean et al., 2020) with the 39.7% deviance explained by primary forest cover (Table 2). Shchuchye Lake demonstrates phased fire regime: strong charcoal pulse at ~12-~11 cal. kyr BP and late-Holocene intensification (Fig. 4c). Key fire events in Ulukh- Chayakh mire occurred in the last millennium and at ~4.5-~3 cal. kyr BP (Fig. 4c).

Cross-site synthesis of fire regimes in the west Siberian plain exhibits three distinct fire phases. In details, burning pulse (only in Shchuchye Lake) at ~12-~11 cal.

https://doi.org/10.5194/egusphere-2025-1991
Preprint. Discussion started: 26 May 2025


kyr BP might be related with the meltwater-mediated charcoal deposition (Blyakharchuk et al., 2024). The Pre-Holocene permafrost maintained waterlogged soils, suppressing ignitions. With disappearance of permafrost soils became drier and fires spread more easy when the time transited into the warming Holocene (Blyakharchuk et al., 2024). The second higher biomass burning at ~8.5-~6 cal. kyr BP was showed in Rybnaya peat, which is related with precipitation-driven higher *Larix* pollen (Feurdean et al., 2022; Zhang and Zhang, 2025). The ~4.2 cal kyr BP burning maximum across all sites coincides with regional megadrought conditions (Feurdean et al., 2022) and emergent pastoralist fire use (Li et al., 2024). The GAMs analysis reveal the divergent fire-vegetation relationships: (1) Negative correlation at Rybnaya/Plotnikovo (canopy >75%): Reduced understory fuels and microclimatic humidity limit fire spread; (2) Positive correlation at Shchuchye Lake (canopy <65%): Open structure promotes flammable grass undergrowth.

**4.2.3. Northern Altai Mountains (Region C, n=4):**

Chudnoye Mire is situated in a remote mountain taiga near the upper limit of the forest (Fig. 1). This region experienced a decline in biomass burning during the early to mid-Holocene, followed by an intensification in the late Holocene (Fig. 4d). Biomass burning can often explain the changes in dominant tree species within mountain forests, particularly the positive correlation observed in *Larix* and *Picea* pollen (Table 2). Tundra mire is characterized by dense forests of *Abies* and *Betula*, as reflected in the pollen data. The charcoal influx exhibited a decreasing trend prior to ~4 cal. kyr BP, after which it began to increase. Mokhovoe Bog, which is covered by birch forest-steppe, shows four peaks in charcoal influx at approximately ~11.5-~9.5 cal. kyr BP, ~8.5-~7 cal. kyr BP, ~5.6-~4 cal. kyr BP, and ~1.5-~1 cal. kyr BP. The only statistical connection between *Picea* and biomass burning may be attributed to increased bioproductivity of the landscape and the availability of fuel due to a more humid climate. Kuatang Lake is located in dark coniferous wet mountain taiga, where the charcoal influx has shown a clear increase since ~3.5 cal. kyr BP, followed by a decreasing trend (Fig. 4d). The positive correlation between charcoal influx and *Betula* pollen, contrasted with the negative correlations with *Abies, P. sibirica* and *P.*

https://doi.org/10.5194/egusphere-2025-1991
Preprint. Discussion started: 26 May 2025


*sylvestris*, suggests that the increased charcoal influx since ~3.5 cal. kyr BP may be attributed to the expansion of birch forest.

The regional synthesis of biomass burning reveals two distinct trends during the Holocene: a gradual decline in the early to mid-Holocene, followed by an increase in the late Holocene that subsequently exhibited a downward trajectory. Elevated charcoal influx in the early to mid-Holocene was predominantly recorded at Chudnoye Mire, Mokhovoe Bog and Tundra Mire. Notably, Mokhovoe Bog demonstrates a 2.1-fold higher charcoal influx compared to Chudnoye Mire and Tundra Mire, likely attributable to its ecotonal position within the forest-steppe transition zone, where progressive vegetation expansion during the early Holocene enhanced fuel availability. The increase in charcoal influx during the late Holocene, observed across all four sites, correlates with regional climatic humidification and intensified anthropogenic activities (Blyakharchuk et al., 2023; Li et al., 2024). Of particular significance, Mokhovoe Bog exhibits the most pronounced charcoal fluxes, reflecting persistent human occupation of these resource-rich landscapes since the Mesolithic era (Blyakharchuk, 2022).

#### 4.2.4. Central Altai Mountains within the forest zone (Region D, n=3):

Holocene biomass burning exhibited an increasing trend in Kendegelukol Lake, Uzunkol Lake and Dzhangyskol Lake (Fig. 4e), with a notably pronounced expansion occurring in the late Holocene. A particularly strong increase in biomass burning was observed since ~1.2 cal. kyr BP in Uzunkol Lake and since ~0.5 cal. kyr BP in Dzhangyskol Lake. Notably, Uzunkol Lake recorded higher levels of biomass burning at ~9.5-~9 cal. kyr BP, coinciding with the transition from a dominant steppe landscape to a forest landscape; however, biomass burning did not maintain elevated levels following this transition (Blyakharchuk et al., 2004). The abnormal peak in charcoal influx at ~9.5-~9 cal. kyr BP was likely caused by an unstable fire regime during the onset of forested landscapes, which were particularly susceptible to ignition due to the prevailing dry climate and the increased availability of fuel from the spread of trees and shrubs (Blyakharchuk & Pupysheva, 2022). Following this transition, biomass burning at Uzunkol Lake decreased, indicating a shift to a more

https://doi.org/10.5194/egusphere-2025-1991
Preprint. Discussion started: 26 May 2025


stable climate and a reduction in fire frequency (Blyakharchuk et al., 2004). In contrast, Kendegelukol Lake and Dzhangyskol Lake exhibited only a slight increase in biomass burning, suggesting that Uzunkol Lake may be more sensitive to local fires due to its location in the forest-steppe transition zone. This observation is supported by similar research indicating that the forest-wooded grassland ecotone was highly sensitive to climate variability during the Holocene (Lezine et al., 2023).

Despite minor variations in early Holocene biomass burning, these three lakes demonstrate a statistically significant intensification of fire activity at ~4.5 cal. kyr BP, with particularly pronounced amplification during the last millennium (Blyakharchuk & Pupysheva, 2022). GAMs analysis reveals strong positive associations between biomass burning and the pollen abundances of *Abies*, *Betula* and *P. sylvestris* across these sites (Table 2), suggesting that fuel-load accumulation through late-Holocene forest expansion drove shifts in fire regimes. The anomalous surge in biomass burning post-1.0 cal. kyr BP likely reflects synergistic anthropogenic drivers, including intensified pastoral burning practices and land clearance (Blyakharchuk et al., 2004, 2008). The regional synthesis demonstrates a sustained upward trajectory in biomass burning throughout the Holocene, culminating in a 2.3-fold increase over the past two millennia relative to early Holocene baselines.

#### 4.2.5. Central Altai Mountains above the forest limit (Region E, n=3):

Regional integrated Z-scores indicate a consistent decline in biomass burning prior to ~2 cal. kyr BP, followed by a rapid increase thereafter (Fig. 4f). GAMs reveal that *Picea* in Tashkol Lake, *Picea* and *P. sylvestris* in Akkol Lake, and *Larix* and *Picea* in Grusha Lake were the primary materials for biomass combustion (Table 2). Significant differences in biomass burning were observed among the three lakes.

Tashkol Lake, situated above the modern forest limit at 2150 m a.s.l., was covered by ice during the glacial period (Blyakharchuk et al., 2004). The sharp peak in charcoal influx around ~11-~10.5 cal. kyr BP was likely caused by the redeposition of microcharcoal by glacial meltwaters (Blyakharchuk et al., 2004). Subsequently, the forested landscapes of central Altai between ~10.5 and ~4 cal. kyr BP, along with late Holocene cooling, are clearly reflected in the biomass burning patterns of Tashkol

https://doi.org/10.5194/egusphere-2025-1991
Preprint. Discussion started: 26 May 2025


Lake, indicating the climate-dependent changes in bioproductivity and fuel availability in high-elevation landscapes. The exceptionally high rate of charcoal influx during the late glacial period, around 12-11 cal. kyr BP, can be attributed to the allochthonous origin of redeposited old charcoal in Grusha Lake (Blyakharchuk et al., 2004). Given that Grusha Lake is located at a high elevation (2413 m a.s.l.) and was covered by glaciers during the glacial period (Rudoy and Yatsuk, 1986), microcharcoal particles accumulated on the glacier surface throughout the glaciation. As the glacier melted, these microcharcoal particles were washed into the lake basin by meltwater. This hypothesis is supported by the very high rate of sediment accumulation in Grusha Lake around ~12-~11 cal. kyr BP (Blyakharchuk et al., 2007). Following deglaciation, the previously bare areas became vegetated, leading to a sharp decrease in the redeposition of microcharcoal at ~10.5 cal. kyr BP. The overall trend of charcoal influx in Akkol Lake is similar to that of Grusha Lake, with the exception of the absence of a peak around ~12-~11 cal. kyr BP. This discrepancy can be explained by the lower-elevation Akkol Lake, where glacial cover was absent, resulting in drier conditions and a lack of redeposited microcharcoal following deglaciation (Blyakharchuk et al., 2007).

**4.2.6. Western Sayan Mountains (Region F, n=3):**

Three peat cores — Lugovoe Peat, Bezrybnoye Mire and Buibinskoye Mire — exhibited a decreasing trend in biomass burning throughout the Holocene (Fig. 4g). In Buibinskoye Mire, a peak in biomass burning is observed around ~12-~11 cal. kyr BP. During the late glacial and early Holocene, permafrost likely extended into the soils, allowing only *Picea* to thrive in the Western Sayan (Blyakharchuk et al., 2022). As permafrost receded, the prevalence of *Picea* diminished, giving way to *P. sibirica* and *Abies*. Following the onset of forestation around ~11 cal. kyr BP, a sharp increase in biomass burning occurred. However, prior to this, between ~11.5 and ~11 cal. kyr BP, intense fires devastated spruce forests. Charcoal influx from three sites demonstrated a similar trend of increase between ~10.5 and ~7 cal. kyr BP, followed by a gradual decline in the late Holocene. The warmer climate during the Holocene climatic optimum likely enhanced the bioproductivity of mountain forests in the Western

https://doi.org/10.5194/egusphere-2025-1991
Preprint. Discussion started: 26 May 2025


Sayan, resulting in increased fuel availability for fires (Blyakharchuk et al., 2013, 2022). The dominance of fire-avoiding *Abies* contributed to the elevated levels of biomass burning during this period. With the onset of late Holocene cooling after ~7 cal. kyr BP, the rate of biomass burning decreased.

The three sites in the Western Sayan Mountains are situated between the upper and lower limits of forest, leading to similar trends in the composition and content of primary forest cover throughout the Holocene (Blyakharchuk et al., 2013, 2022). The GAMs results indicate that *Abies* and *Larix* in Lugovoe Mire are the primary contributors to biomass burning, while *Abies* in Buibinskoye Mire also plays a significant role (Table 2). Although no significant relationship was found between biomass burning and vegetation in Bezrybnoye Mire, the fire-resistant species *P. sylvestris* (Feurdean et al., 2022) accounted for the largest deviance explanation (28.10%) for biomass burning (Table 2). This suggests that the expansion of *P. sylvestris* forests led to a reduction in the area of other combustible materials, supported by the negative correlation between the spread of *P. sylvestris* and the decrease in biomass combustion in Lugovoe Mire and Buibinskoye Mire (Table 2). Consequently, the fire-resistant *P. sylvestris* can proliferate in the piedmonts of the Western Sayan Mountains at the expense of fire-avoiding *Abies*. The dominance of fire-resistant *P. sylvestris* has contributed to the reduction of biomass burning in the forested areas of the Western Sayan.

#### 4.2.7. Khangai Mountains (Region G, n=3):

Higher biomass burning was observed between ~3.5 and ~3.1 cal. kyr BP in Olgi Lake (2012 m a.s.l.), between ~3.7 and ~3.3 cal. kyr BP in Shireet Naiman Nuur (2429 m a.s.l.), and between ~2.4 and ~2.1 cal. kyr BP in Ugii Nuur (1330 m a.s.l.) (Fig. 4h). Pollen data suggest that forest vegetation currently exists only at lower elevations in the Khangai Mountains, while higher elevations remain devoid of forest cover (Unkelbach et al., 2021; Barhoumi et al., 2024; Wang et al., 2011). Ugii Nuur exhibited significantly higher biomass burning than both Olgi Lake and Shireet Naiman Nuur, likely due to greater steppe vegetation coverage at lower elevations, which provided abundant burning sources and stronger human influence around

https://doi.org/10.5194/egusphere-2025-1991
Preprint. Discussion started: 26 May 2025


~2.4-~2.1 cal. kyr BP (Wang et al., 2011). Although Shireet Naiman Nuur recorded a gradual decline in biomass burning during the middle and late Holocene, its charcoal influx was considerably lower than that of Olgi Lake and Ugii Nuur (Fig. 4h). The charcoal data from high-elevation Shireet Naiman Nuur may reflect only climate-induced decreases in biomass burning (late Holocene cooling), whereas the charcoal data from Olgi Lake and Ugii Nuur indicate clear human influence around ~3.4-~3.1 cal. kyr BP and ~2.4-~2.1 cal. kyr BP, respectively. The GAMs analysis revealed that biomass burning in Olgi Lake was negatively correlated with primary forest cover and other woody types (Fig. S8), suggesting that biomass burning around Olgi Lake was primarily controlled by herbaceous-dominated steppe vegetation. In contrast, biomass burning in Shireet Naiman Nuur and Ugii Nuur was positively correlated with primary forest cover and other woody types, indicating that biomass burning in these areas was mainly regulated by woody vegetation, with *P. sibirica* having the highest explanatory power (Table 2). According to pollen data, forests also existed at high elevations near Shireet Naiman Nuur (2429 m a.s.l.) between ~7.5 and ~4 cal. kyr BP, but did not grow near Olgi Lake (2012 m a.s.l.) (Unkelbach et al., 2021; Barhoumi et al., 2024). During the middle Holocene optimum, some high-elevation areas of the Khangai Mountains were covered by forests with high bioproductivity, which contributed to increased biomass burning. However, the Khangai Mountains gradually deforested during the late Holocene, leading to a decrease in biomass burning to present low levels (Unkelbach et al., 2021; Barhoumi et al., 2024; Wang et al., 2011).

The role of *Picea* near Olgi Lake was more significant during the early Holocene (~9.5-~8.5 cal. kyr BP), decreased during the period from ~8.5 to ~2 cal. kyr BP, and then increased again after ~1.5 cal. kyr BP (Unkelbach et al., 2021; Barhoumi et al., 2024). This fluctuation may be attributed to increased humidity, as *Picea* requires wetter soils than *Pinus* (Blyakharchuk et al., 2013). The maximum charcoal influx around ~3-~4 cal. kyr BP may be linked to early human influence (Xiang et al., 2023) or to climatic shifts during the mid-Holocene transition (Zhao et al., 2017). This climatic shift may have caused intense fires across all areas of the Khangai, resulting in widespread deforestation. This hypothesis is supported by the decrease in the

https://doi.org/10.5194/egusphere-2025-1991
Preprint. Discussion started: 26 May 2025


contents of forest pollen in Shireet Naiman Nuur following the charcoal maximum around ~3-~4 cal. kyr BP (Barhoumi et al., 2024).

### 4.3. Holocene climate-fuel feedbacks across the different regions

The relatively low biomass burning in the southeastern/western Altai Mountains within the steppe zone prior to the last 2000 years coincided with low vegetation cover (Sun et al., 2013; Hu et al., 2024; Li et al., 2021; Rudaya et al., 2020), indicating that the drought-induced low vegetation cover inhibits fire occurrence (Zhang et al., 2022). Since the last 2000 years, the rapid increase in biomass burning has been attributed to changing climate conditions and intensified human activities (Hu et al., 2024; Tian et al., 2021; Zhang and Zhang, 2025; Rudaya et al., 2020). A similar pattern of low biomass burning prior to the last 2000 years was recorded in the central Altai Mountains within the forest zone, including Kendegelukol, Uzunkol and Dzhangyskol Lake. In Kendegelukol and Uzunkol Lake, forest components exceeding 70% suggest that dense forest coverage in the surrounding landscapes may limit biomass burning (Carter et al., 2020). In Dzhangyskol Lake, situated in the forest-steppe transition zone, the sustained low biomass burning before the last 2000 years may be attributed to lower vegetation productivity (Blyakharchuk et al., 2004, 2008). The significant increase in biomass burning over the past 2000 years across these records may be directly related to intensified cattle grazing and human settlement (Feurdean et al., 2020; Li et al., 2024; Rudaya et al., 2020; Xiang et al., 2023; Zhang et al., 2022). Increased biomass burning around ~4.5-~3 cal. kyr BP may be linked to human influence, as indicated by the presence of Triticum pollen (Blyakharchuk et al., 2004, 2008). These findings are associated with the development of ancient cultures (Blyakharchuk et al., 2004, 2008; Xiang et al., 2024).

In stark contrast to the trends observed in the first two regions, biomass burning has shown an overall decline since the Holocene in the central Altai Mountains above the forest limit, the western Sayan Mountains and the Khangai Mountains. The gradual decrease in biomass burning above the timberline in the central Altai Mountains is primarily influenced by the response of forest vegetation cover to temperature changes. In the Western Sayan Mountains, the main forest vegetation

https://doi.org/10.5194/egusphere-2025-1991
Preprint. Discussion started: 26 May 2025


cover exceeds 80%, indicating that material availability is not a limiting factor for regional biomass burning. The GAMs analysis reveals that the decline in biomass burning in the Sayan Mountains is significantly associated with changes in forest composition. Specifically, the increase in Siberian pine and European larch since the Holocene has led to a significant decline in fir, birch, larch, and spruce components, resulting in a notable decrease in combustible materials at the three sites. Therefore, the decline in Holocene biomass in the Sayan region is primarily driven by changes in forest composition under temperature regulation. Notably, unlike the gradual increase in Holocene biomass burning observed in Kendegelukol and Uzunkol Lake, which are also in forested regions, there has been no overall decline in the Sayan region. This discrepancy is primarily attributed to human activities that have altered the occurrence of regional fires.

Although Holocene biomass burning in the Khangai Mountains exhibits an overall gradual decline, it can be categorized into two distinct phases: an increase over the past 2,000 years, followed by a gradual decline post-2000 year (Unkelbach et al., 2021; Barhoumi et al., 2024). The biomass burning characteristics during the earlier phase resemble those observed in the southeastern and western Altai Mountains, primarily due to increased humidity in the region, which led to a rise in combustible materials. In the later phase, despite the humid climate, the absence of a significant increase in biomass burning in the Khangai Mountains may be attributed to human grazing activities that have fragmented surface vegetation (Zhang S.J. et al., 2021). This assertion is supported by the studies of modern landscape, where livestock grazing eliminates most of the fuels necessary to sustain a fire (Umbanhowar et al., 2009; Zhang et al., 2022). The impact of human activities is also evident in areas above the timberline in the central Altai Mountains and the Sayan Mountains; however, the timing of this impact in the central Altai Mountains (~2.5 cal. kyr BP) predates that in the Sayan Mountains (~1 cal. kyr BP).

Biomass burning in the northern Altai Mountains demonstrates a gradual decline during the early to middle Holocene (Fig. 4d), a pattern consistent with trends observed above the upper forest line in the central Altai Mountains and the Sayan

https://doi.org/10.5194/egusphere-2025-1991
Preprint. Discussion started: 26 May 2025


Mountains (Fig. 4f-g). This early to mid-Holocene decline is likely related to temperature-regulated forest vegetation dynamics. The late-Holocene increase in biomass burning is associated with the intensified anthropogenic disturbances (Blyakharchuk et al., 2024; Blyakharchuk, 2022). The West Siberian Plain exhibits four peaks of Holocene biomass burning at ~12-~11 cal. kyr BP, ~8.4-~6.6 cal. kyr BP, ~4.4-~4.2 cal. kyr BP and ~1.4 cal. kyr BP (Fig. 2c). The first peak recorded at Shchuchye Lake derived from ancient sediments in formerly glaciated or permafrost-affected areas (Blyakharchuk et al., 2024). The second peak at Rybnaya Peat corresponds to high *Larix* coverage around the mire (Feurdean et al., 2022). The third peak is supported by biomass burning from the southeastern and western Altai, central Altai, Sayan and Khangai Mountains, potentially linked to regional aridity or increased human activity (Zhang and Zhang, 2025). Notably, a Bronze Age charcoal pulse (~4-~3 cal. kyr BP) at Kuatang Bog and an Early Iron Age pulse (~3 cal. kyr BP) at Tundra Mire coincide with the Kuznetski Alatau Mountains—a known center of ancient Siberian metallurgy (Slavnin and Sherstova, 1999). The fourth peak directly corresponds to numerous archaeological sites of ancient human cultures, indicating densely populated areas (Panyushkina, 2012; Agatova et al., 2014; Xiang et al., 2024).

## 5. Conclusions

This study presents a long-term fire record from the steppe zone of Western Mongolia and evaluates the spatial variations in biomass burning and its relationship with forest composition across the Altai-Sayan Mountains and adjacent plains. Our findings indicate that the reduction in biomass burning during the Holocene can be attributed to the temperature-regulated woody biomass above the forest limit in the central Altai Mountains, as well as a decrease in combustible components (*Larix*, *Abies* and *Picea*) in the western Sayan Mountains and northern Altai Mountains. Global cooling and increased moisture during the late Holocene contributed to the declining trend of biomass burning in the western Sayan Mountains and central Altai Mountains within the forest zone. A notable increase in biomass burning since ~4 cal. kyr BP has been observed in areas historically populated by various archaeological cultures. The late Holocene rise in biomass burning occurred in regions that were previously less susceptible to fires due to either excessively wet and cool climates (such as the plains and mountain taiga of Western Siberia and the Altai Mountains) or excessively dry climates with sparse steppe or desert-steppe vegetation that could not provide sufficient fuel for fires. The latter scenario is characteristic of southeastern Altai, particularly in the steppe areas surrounding Kuchuk Lake, as well as in Uzunkol and Dzhangyskol lakes located in intermountain hollows covered by steppe vegetation. Intensified human activities, including agriculture and pasture, have led to increased fire frequency since ~2 cal. kyr BP in the southeastern Altai Mountains, the West Siberian Plain, and the forest zone of the middle Altai Mountains. Conversely, the significant decline in biomass burning in the Khangai Mountains may be attributed to vegetation fragmentation caused by grazing activities. This research elucidates the long-term relationship between biomass burning and forest composition/density across different vegetation zones in the Altai-Sayan Mountains and adjacent plains, which holds practical significance for predicting and managing future fire dynamics.

**CRediT authorship contribution statement**

Dongliang Zhang: Writing – review & editing, Validation, Methodology, Funding acquisition, Conceptualization. Blyakharchuk Tatiana, Aizhi Sun, Xiaozhong Huang: Writing – original draft, Visualization, Methodology, Data curation. Yuejing Li – Data curation.

**Declaration of Competing Interest**

The authors declare that they have no known competing financial interests or personal relationships that could have appeared to influence the work reported in this paper.

**Acknowledgment.** This research was financially supported by National Natural Science Grants of China (No. 42471183), Youth Innovation Promotion Association of Chinese Academy of Sciences (No. 2022447) and National Natural Science Grants of China (No. 42220104001). We thank anonymous reviewers for their valuable comments, which significantly improved the manuscript.

**References**

Agatova, A.R., Nepop, R.K., Bronnikova, M.A., Slyusarenko, I.Tu., Orlova, L.A. Human occupation of South Eastern Altai highlands (Russia) in the context of

https://doi.org/10.5194/egusphere-2025-1991
Preprint. Discussion started: 26 May 2025


Environmental changes. Archaeological and Anthropological Sciences. DOI 10.1007/s12520-014-0202-7.

Albrich, K., Rammer, W., Thom, D., Seidl, R., 2018. Trade-offs between temporal stability and level of forest ecosystem services provisioning under climate change. Ecological Applications, 28(7), 1884-1896.

Andela, N., Morton, D.C., Giglio, L., Chen, Y., van der Werf, G.R., Kasibhatla, P.S., DeFries, R.S., Collatz, G.J., Hantson, S., Kloster, S., Bachelet, D., Forrest, M., Lasslop, G., Li, F., Mangeon, S., Melton, J.R., Yue, C., Randerson, J.T., 2017. A human-driven decline in global burned area. Science, 356, 1356-1362.

Archibald, S., Lehmann, C. E., Gómez-Dans, J.L., Bradstock, R.A., 2013. Defining pyromes and global syndromes of fire regimes. PNAS, 110(16), 6442-6447.

Barhoumi, C., Bliedtner, M., Zech, R., Behling, H., 2024. Holocene vegetation, fire, climate dynamics and human impact in the upper Orkhon Valley of the Khangai Mountains, Mongolia. Quat. Sci. Rev. 334, 108713.

Barhoumi, C., Bliedtner, M., Zech, R., Behling, H., 2024. Holocene vegetation, fire, climate dynamics and human impact in the upper Orkhon Valley of the Khangai Mountains, Mongolia. Quat. Sci. Rev. 334, 108713.

Bezrukova, E.V., Abzaeva, A.A., Letunova, P.P., Kulagina, N.V., Vershinin, A.V., Belov, A.V., Orlova, L.A., Danko, L.V., Krapivina, S.M., 2005. Post-glacial history of Siberian spruce (Picea obovate) in the lake Baikal area and the significance of this species as a paleo-environmental indicator. Quaternary International 136, 47-57. DOI: 10.1016/j.quaint.2004.11.007.

Blyakharchuk, T.A., Wright, H.E., Borodavko, P.S., van der Knaap, W.O., Ammann, B., 2004. Late Glacial and Holocene vegetational changes on the Ulagan high-mountain plateau, Altai Mountains, southern Siberia. Palaeogeography, Palaeoclimatology, Palaeoecology, 209(1-4), 259-279.

Blyakharchuk, T.A., Wright, H.E., Borodavko, P.S., van der Knaap, W.O., Ammann, B., 2007. Late glacial and Holocene vegetational history of the Altai mountains (southwestern Tuva Republic, Siberia). Palaeogeography, Palaeoclimatology, Palaeoecology, 245(3-4), 518-534.

https://doi.org/10.5194/egusphere-2025-1991
Preprint. Discussion started: 26 May 2025


Blyakharchuk, T.A., Wright, H.E., Borodavko, P.S., van der Knaap, W.O., Ammann, B., 2008. The role of pingos in the development of the Dzhangyskol lake-pingo complex, central Altai Mountains, southern Siberia. Palaeogeography, Palaeoclimatology, Palaeoecology, 257(4), 404-420.

Blyakharchuk, T.A., Chernova, N.A., 2013. Vegetation and climate in the Western Sayan Mts according to pollen data from Lugovoe Mire as a background for prehistoric cultural change in southern Middle Siberia. Quat. Sci. Rev. 75, 22-42.

Blyakharchuk, T.A., Kuryina, I.V., Pologova, N.N., 2019. Late Holocene dynamics of vegetation cover and climate humidity in the southeastern sector of the West Siberian Plain according to palynological and rhizopod studies of peat deposits. Bulletin of Tomsk State University. Biology 45, 164–189. (in Russian)

Blyakharchuk, T.A., Pupysheva, M.A., 2022. Indication of fires in the thousand-year history of Central Altai. Geography and Natural Resource, 4, 128-136 (In Russian).

Blyakharchuk, T.A., van Hardenbroek, M., Pupysheva, M.A., Kirpotin, S.N., Blyakharchuk, P.A., 2024. Late Glacial and Holocene history of climate, vegetation landscapes and fires in South Taiga of Western Siberia based on radiocarbon dating and multi-proxy palaeoecological research of sediments from Shchuchye Lake. Radiocarbon, 1-24, doi:10.1017/RDC.2024.103.

Blyakharchuk, T.A., 2020. Dynamics of vegetation cover and quantitative palaeoclimatic reconstructions in the Western Sayan Mountains from the Late Glacial period to the present time according to a palynological study of the Yuzhno-Buybinskoe mire. In IOP Conference Series: Earth and Environmental Science (Vol. 611, No. 1, p. 012026). IOP Publishing.

Blaauw, M., Christen, J.A., 2011. Flexible paleoclimate age-depth models using an autoregressive gamma process. Bayesian Analysis 6, 457–474.

Carter, V. A., Bobek, P., Moravcová, A., Šolcová, A., Chiverrell, R. C., Clear, J. L., Kuneš, P., 2020. The role of climate-fuel feedbacks on Holocene biomass burning in upper-montane Carpathian forests. Global and Planetary Change, 193, 103264.

https://doi.org/10.5194/egusphere-2025-1991
Preprint. Discussion started: 26 May 2025


Davis, M.B., 1965. A method for determination of absolute pollen frequency. Handbook of paleontological techniques. San-Francisco-London: Freeman & Co, P. 674–686.

Feurdean, A., Florescu, G., Tanţău, I., Vannière, B., Diaconu, A. C., Pfeiffer, M., Kirpotin, S., 2020. Recent fire regime in the southern boreal forests of western Siberia is unprecedented in the last five millennia. Quat. Sci. Rev. 244, 106495.

Feurdean, A., Diaconu, A.C., Pfeiffer, M., Gałka, M., Hutchinson, S.M., Butiseaca, G., Gorina, N., Tonlkov, S., Niamir, A., Tantau, I., Zhang, H., Kirpotin S., 2022) Holocene wildfire regimes in Western Siberia: Interaction between peatland moisture conditions and the composition of plant functional types. Climate of the Past 18, 1255–1274

Fu, B.J., Liu, G.H., Ouyang, Z.Y., 2013. Ecological regionalization in China. Beijing: Science Press.

Furyaev, V.V., 1996. Role of Fire in Forest Development. Nauka Publications: Novosibirsk (In Russia).

Ivanova, G.A., Kukavskaya, E.A., Ivanov, V.A., Conard, S.G., McRae, D.J., 2020. Fuel characteristics, loads and consumption in Scots pine forests of central Siberia. J. Forestry Res. 31(6), 2507-2524.

Jones, M.W., Smith, A., Betts, R., Canadell, J.G., Prentice, I.C., Le Quéré, C., 2020. Climate change increases the risk of wildfires. ScienceBrief Rev. 116, 117.

Kasischke, E.S., 2000. Boreal ecosystems in the global carbon cycle. In: Kasischke, E.S., Stocks, B.J. (Eds.), Fire, Climate Change, and Carbon Cycling in the Boreal Forest. Ecological.

Kelly, R.F., Higuera, P.E., Barrett, C.M., Hu, F.S., 2011. A signal-to-noise index to quantify the potential for peak detection in sediment–charcoal records. Quat. Res. 75, 11–17.

Khabarov, N., Krasovskii, A., Obersteiner, M., Swart, R., Dosio, A., San-Miguel-Ayanz, J., Migliavacca, M., 2016. Forest fires and adaptation options in Europe. Region. Environ. Chang. 16, 21-30.

Kharuk, V.I., Ponomarev, E.I., Ivanova, G.A., Dvinskaya, M.L., Coogan, S.C., Flannigan, M.D., 2021. Wildfires in the Siberian taiga. Ambio, 50(11),

https://doi.org/10.5194/egusphere-2025-1991
Preprint. Discussion started: 26 May 2025


1953-1974.

Krylov, A., McCarty, J.L., Potapov, P., Loboda, T., Tyukavina, A., Turubanova, S., Hansen, M.C., 2014. Remote sensing estimates of stand-replacement fires in Russia, 2002-2011. Environ. Res. Lett. 9(10), 105007.

Goldammer, J.G., Furyaev, V., 2013. Fire in ecosystems of boreal Eurasia (Vol. 48). Springer Science & Business Media.

Hastie, T.J., Tibshirani, R.J., 1986. Generalized additive models. Stat. Sci. 1 (3), 297–318.

Higuera, P.E., Brubaker, L.B., Anderson, P.M., Hu, F.S., Brown, T., 2009. Vegetation mediated the impacts of postglacial climate change on fire regimes in the southCentral Brooks Range, Alaska. Ecol. Monogr. 79, 201–219.

Higuera, P.E., Gavin, D.G., Bartlein, P.J., Hallett, D.J., 2010. Peak detection in sediment–charcoal records: impacts of alternative data analysis methods on fire-history interpretations. Int. J. Wildland Fire 19, 996–1114.

Hu, Y., Huang, X., Demberel, O., Zhang, Jun, Xiang, L., Gundegmaa, V., Huang, C., Zheng, M., Zhang, Jiawu, Qiang, M., Xiao, J., Chen, F., 2024. Quantitative reconstruction of precipitation changes in the Mongolian Altai Mountains since 13.7 ka. Catena 234, 107536.

Huang, X., Peng, W., Rudaya, N., Grimm, E.C., Chen, X., Cao, X., Zhang, J., Pan, X., Liu, S., Chen, C., Chen, F., 2018. Holocene vegetation and climate dynamics in the Altai Mountains and surrounding areas. Geophys. Res. Lett. 45 (13), 6628-6636.

Lézine, A.M., Izumi, K., Achoundong, G., 2023. Mbi Crater (Cameroon) illustrates the relations between mountain and lowland forests over the past 15,000 years in western equatorial Africa. Quat. Int. 657, 67-76.

Li, Y., Zhang, Y., Wang, J., Wang, L., Li, Y., Chen, L., Zhao, L., Kong, Z., 2019. Preliminary study on pollen, charcoal records and environmental evolution of Alahake Saline Lake in Xinjiang since 4,700 cal yr BP. Quat. Int. 513, 8–17.

Li, Y., Zhang, D., Zhang, Y., Sun, A., Li, X., Huang, X., Zhang, Y., Li, Y., 2024. Distentanging the late-Holocene human–environment interactions in the Altai Mountains within the Arid Central Asia. Palaeogeography, Palaeoclimatology,

https://doi.org/10.5194/egusphere-2025-1991
Preprint. Discussion started: 26 May 2025


Palaeoecology, 654, 112466.

Liu, F., Liu, H., Xu, C., Shi, L., Zhu, X., Qi, Y., He, W., 2021. Old-growth forests show low canopy resilience to droughts at the southern edge of the taiga. Global Change Biology, 27(11), 2392-2402.

Lung, T., Lavalle, C., Hiederer, R., Dosio, A., Bouwer, L.M., 2013. A multi-hazard regional level impact assessment for Europe combining indicators of climatic and non-climatic change. Global and Environmental Change, 23, 522-536.

Moritz, M.A., Batllori, E., Bradstock, R.A., Gill, A.M., Handmer, J., Hessburg, P.F., Leonard, J., McCaffrey, S., Odion, D.C., Schonennagel, T., Syphard, A.D., 2014. Learning to coexist with wildfire. Nature, 515(7525), 58-66.

Panyushkina, I.P., 2012. Climate-Induced changes in Population Dynamics of Siberian Scythians (700-250 B.C.). Climate, Landscapes and Civilizations. Geographycal Monograph Series 198, 145-154.

Pitkanen, A., Huttunen, P., Tolonen, K., Jungner, H., 2003. Long term fire frequency in the spruce-dominated forests of the Ulvinsalo strict nature reserve. Finland. Forest Ecology and Management, 176(1-3), 305-319.

Ponomarev, E.I., Kharuk, V.I., 2016. Wildfire occurrence in forests of the Altai-Sayan region under current climate changes. Contemporary Problems of Ecology, 9, 29-36.

Power, M.J., Marlon, J., Ortiz, N., et al., 2007. Changes in fire regimes since the Last Glacial Maximum: an assessment based on a global synthesis and analysis of charcoal data. Climate dynamics, 30, 887-907.

Pupycheva, M.A., Blyakharchuk, T.A., 2024. Late Holocene dynamics of fires in the forest-steppe zone (a case study of the Nikolaevsky Ryam) Geografiya I prirosnye resursy. 1, 54-61 (in Russian).

Reimer, P.J., Austin, W.E., Bard, E., Bayliss, A., Blackwell, P.G., Ramsey, C.B., Talamo, S., 2020. The IntCal20 Northern Hemisphere radiocarbon age calibration curve (0–55 cal kBP). Radiocarbon 62 (4), 725–757.

Rudaya, N., Sergey, K., Michał, S., Xianyong, C., Snezhana, Z., 2020. Postglacial history of the steppe Altai: climate, fire and plant diversity. Quat. Sci. Rev. 249, 106616.

https://doi.org/10.5194/egusphere-2025-1991
Preprint. Discussion started: 26 May 2025


Rudoy, A.N., Yatsuk, T.Yu., 1986. The palaeogeography of southeastern Altai. Chetvertichnaya geologiya i pervobytnaya arkheologiya. Thesis of conference, Ulan-Ude, 73–75.

Shi, C.M., Liang, Y., Gao, C., Wang, Q.H., Shu, L.F., 2020. Drought-modulated boreal forest fire occurrence and linkage with La Nina events in Altai Mountains Northwest China. Atmosphere, 11, 956.

Sun, A., Feng, Z.D., Ran, M., Zhang, C.J., 2013. Pollen-recorded bioclimatic variations of the last ~22,600 years retrieved from Achit Nuur core in the western Mongolian Plateau. Quat. Int. 311, 36-43.

Shi, C.M., Liang, Y., Gao, C., Wang, Q.H., Shu, L.F., 2020. Drought-modulated boreal forest fire occurrence and linkage with La Nina events in Altai Mountains Northwest China. Atmosphere, 11, 956.

Shumilova, L.V., 1962. Botanical Geography of Siberia. Tomsk University Press: Tomsk. (in Russian).

Slavnin, V.D., Sherstova L.I. 1999. Aerchaeologic-Ethnographic Essay of Northern Khakassia in the Area of Geological Polygon of Siberian High School). Tomsl Polytechnical University Press, Tomsk (in Russian)

Stockmarr, J.A., 1971. Tabletes with spores used in absolute pollen analysis. Pollen spores, 13, 61–621.

Tang, G., Yang, S., Miao, Y., et al., 2022. Grain size characteristics of microfossil charcoal and the environmental implications in loess deposits from Ganzi, Western Sichuan Plateau. Journal of Lanzhou University (Natural Sciences) 58 (03), 298–305 (in Chinese with English astract).

Stockmarr J.A., 1971. Tabletes with spores used in absolute pollen analysis. Pollen spores, 13, 61-621.

Umbanhowar Jr, C.E., Shinneman, A.L., Tserenkhand, G., Hammon, E.R., Lor, P., Nail, K., 2009. Regional fire history based on charcoal analysis of sediments from nine lakes in western Mongolia. Holocene 19(4), 611-624.

Unkelbach, J., Dulamsuren, C., Klinge, M., Behling, H., 2021. Holocene high-resolution forest-steppe and environmental dynamics in the Tarvagatai Mountains, northcentral Mongolia, over the last 9570 cal yr BP. Quat. Sci. Rev.

https://doi.org/10.5194/egusphere-2025-1991
Preprint. Discussion started: 26 May 2025


266, 107076.

Walker, X.J., Baltzer, J.L., Cumming, S.G., Day, N.J., Ebert, C., Goetz, S., Johnstone, J.F., Potter, S., Rogers, B.M., Schuur, E.A.G., Turetsky, M.R., Mack, M.C., 2019. Increasing wildfires threaten historic carbon sink of boreal forest soils. Nature, 572, 520-523.

Wang, W., Ma, Y.Z., Feng, Z.D., Narantsetseg, Ts, Liu, K.B., Zhai, X.W., 2011. A prolonged dry mid-Holocene climate revealed by pollen and diatom records from Lake Ugii Nuur in central Mongolia. Quat. Int. 229 (1e2), 74-83.

Wang, Z., Miao, Y., Zhao, Y., Zhang, Z., Zou, Y., Zhang, T., 2024. Preliminary exploration of the fire activity recorded by microcharcoal in surface sediments of Central and Western China. Quat. Sci. 44 (1), 201-213 (in Chinese with English astract).

Wood, S.N., 2017. Generalized Additive Models: An Introduction with R (2nd Edition). Chapman and Hall/CRC, pp1-476.

Xiao, Y., Xiang, L., Huang, X., et al., 2021. Moisture changes in the Northern Xinjiang Basin over the past 2400 years as Documented in Pollen Records of Jili Lake. Front. Earth Sci. 9, 741992.

Xiang, L., Huang, X., Sun, M., Panizzo, V. N., Huang, C., Zheng, M., Chen, F., 2023. Prehistoric population expansion in Central Asia promoted by the Altai Holocene climatic optimum. Nature Communications, 14(1), 3102.

Xinjiang Comprehensive Expedition Team, Institute of Botany, Chinese Academy of Sciences, 1978. Vegetation and its utilization in Xinjiang. Beijing: Science Press.

Zhang, D.L., Feng, Z.D., 2018. Holocene climate variations in the Altai Mountains and the surrounding areas: a synthesis of pollen records. Earth Sci. Rev. 185, 847-869.

Zhang, D., Huang, X., Liu, Q., Chen, X., Feng, Z., 2022. Holocene fire records and their drivers in the westerlies-dominated Central Asia. Sci. Total Environ. 833, 155153.

Zhang, S.J., Lu, Y., Wei, W., Qiu, M., Dong, G., Liu, X., 2021. Human activities have altered fire-climate relations in arid Central Asia since ~1000 a BP: evidence from a 4200-year-old sedimentary archive. Sci. Bull. 66(8), 761-764.

https://doi.org/10.5194/egusphere-2025-1991
Preprint. Discussion started: 26 May 2025


Zhang, Y.Y., Feng, Z.D., 2024. Pollen-based quantitative reconstructions of Holocene climate at Gun Nuur in the northern Mongolian Plateau. Palaeogeography, Palaeoclimatology, Palaeoecology, 638, 112028.

Zhang, Y.Y., Zhang, D.L., 2025. Spatiotemporal patterns of pollen-based Holocene precipitation variations in the Altai Mountains and the surrounding areas. Global and Planetary Change, 251, 104832.

Zhao, Y., Liu, Y.L., Guo, Z.T., Fang, K.Y., Li, Q., Cao, X.Y., 2017. Abrupt vegetation shifts caused by gradual climate changes in central Asia during the Holocene. Sci. China Earth Sci. doi: 10.1007/s11430-017-9047-7

https://doi.org/10.5194/egusphere-2025-1991
Preprint. Discussion started: 26 May 2025


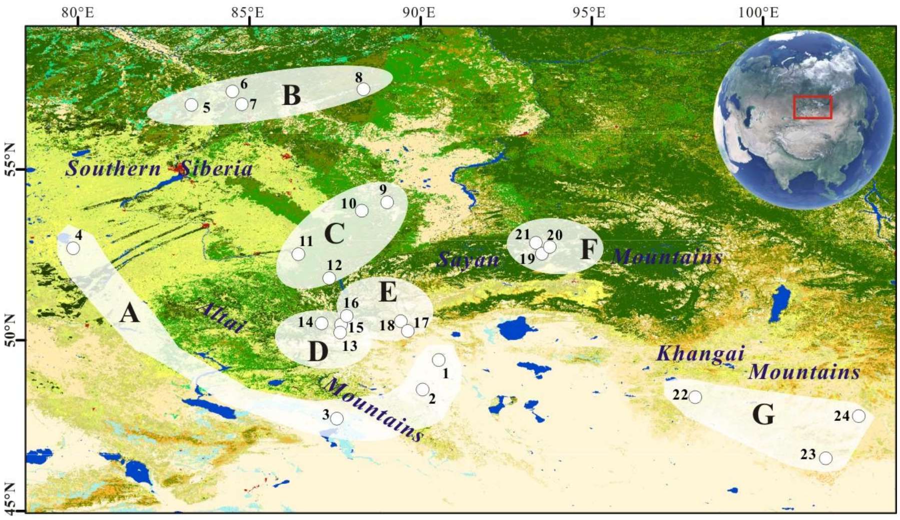


**Fig. 1.** Spatial distributions of the selected fossil pollen/charcoal sequences around the Altai-Sayan Mountains and adjacent plains. **Region A**: Achit Nuur (1), Tolbo Lake (2), Alahake Lake (3) and Kuchuk Lake (4); **Region B**: Rybnaya Mire (5), Plotnikovo Mire (6), Shchuchye Lake (7) and Ulukh–Chayakh Mire (8); **Region C**: Chudnoye Mire (9), Tundra Mire (10), Mokhovoe Bog (11) and Kuatang Mire (12); **Region D**: Dzhangyskol Lake (13), Uzunkol Lake (14) and Kendegelukol Lake (15); **Region E**: Tashkol Lake (16), Akkol Lake (17) and Grusha Lake (18); **Region F**: Buibinskoye Mire (19), Bezrybnoye Mire (20) and Lugovoe Peat (21); **Region G**: Olgi Lake (OL3) (22), Shireet Naiman Nuur (23) and Uggi Nuur (24).

.

https://doi.org/10.5194/egusphere-2025-1991
Preprint. Discussion started: 26 May 2025


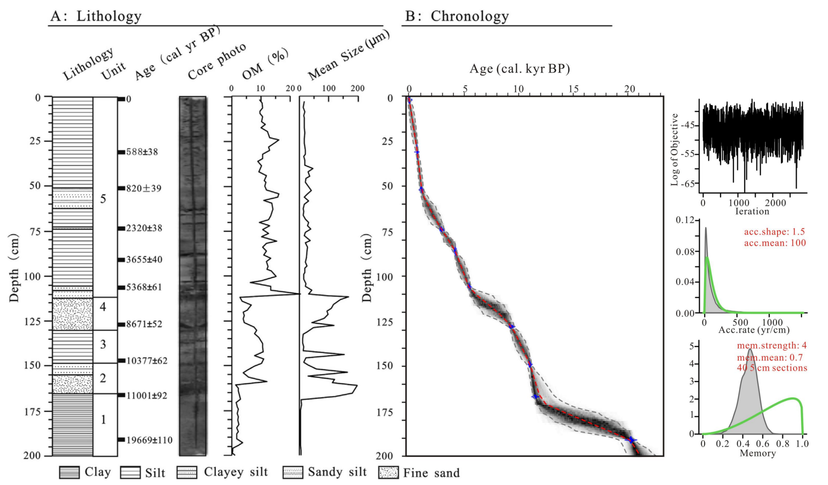


**Fig. 2.** Lithology, core photo, organic matter (OM), mean grain size and depth-age model in Achit Nuur (modified from Sun et al., 2023).

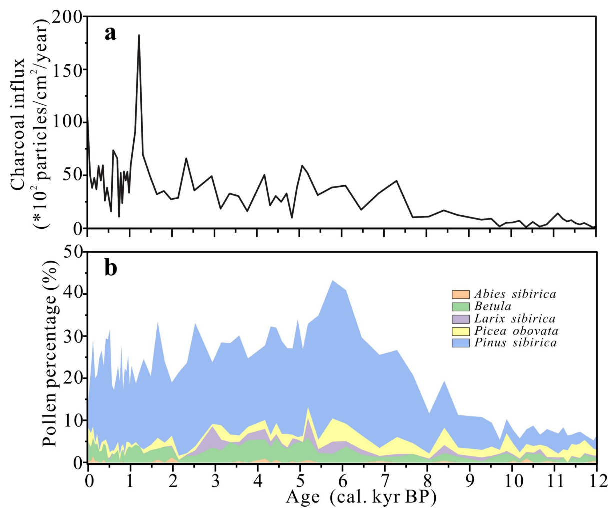


**Fig. 3.** Achit Nuur: biomass burning indicated by charcoal influx (a), vegetation change (b) (Sun et al., 2013; this study).

https://doi.org/10.5194/egusphere-2025-1991
Preprint. Discussion started: 26 May 2025


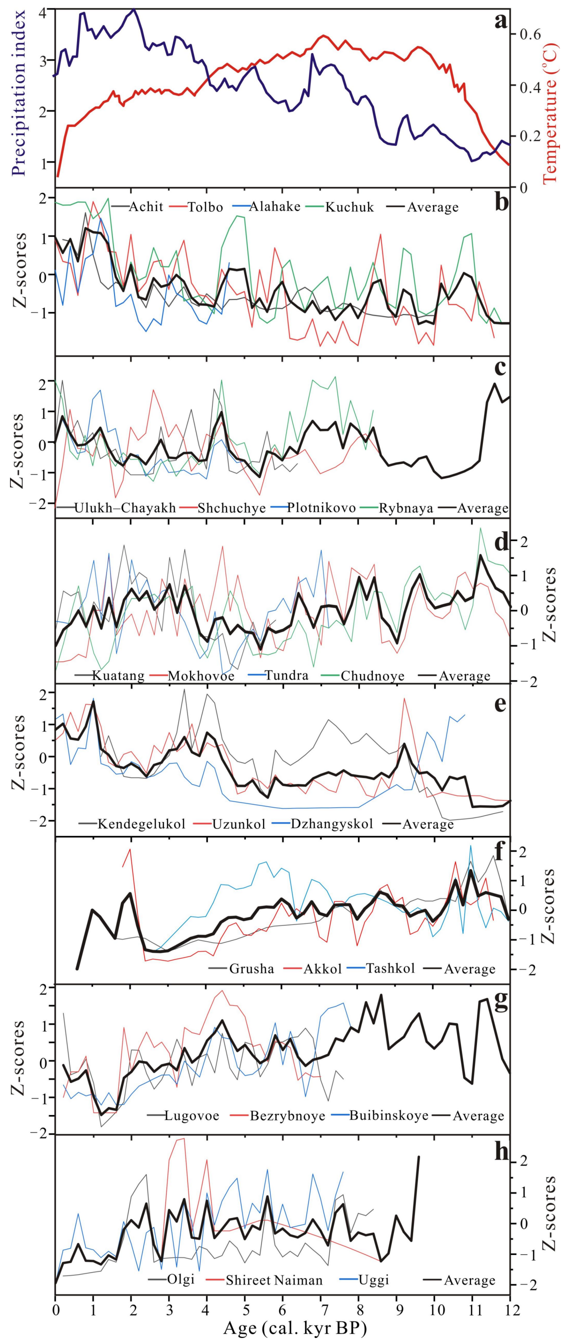


**Fig. 4.** Regional integrated biomass burning (b-g) under the context of temperature (Marcott et al., 2013) and precipitation index (a) in the Holocene interval (Zhang and Feng, 2018).

https://doi.org/10.5194/egusphere-2025-1991
Preprint. Discussion started: 26 May 2025


**Table 1** Detailed information of the selected sites around the Altai-Sayan Mountains and adjacent plains.

| Region | No. | Site Name | Lat. (N) | Long. (E) | Elev. (m a.s.l.) | References |
|---|---|---|---|---|---|---|
| A | 1 | Achit Nuur | 49.42 | 90.52 | 1444 | Sun et al., 2013; this study |
| | 2 | Tolbo Lake | 48.55 | 90.05 | 2080 | Hu et al., 2024 |
| | 3 | Alahake Lake | 47.69 | 87.54 | 483 | Li et al., 2021 |
| | 4 | Kuchuk Lake | 52.69 | 79.84 | 98 | Rudaya et al., 2020 |
| B | 5 | Rybnaya Mire | 57.28 | 84.49 | - | Feurdean et al., 2022 |
| | 6 | Plotnikovo Mire | 56.88 | 83.30 | 120 | Feurdean et al., 2020 |
| | 7 | Shchuchye Lake | 57.13 | 84.61 | 80 | Blyakharchuk et al., 2024 |
| | 8 | Ulukh–Chayakh Mire | 57.34 | 88.32 | - | Feurdean et al., 2022 |
| C | 9 | Chudnoye Mire | 54.03 | 89.01 | 1147 | Blyakharchuk et al., 2024 |
| | 10 | Tundra Mire | 53.79 | 88.27 | 247 | Blyakharchuk et al., 2024 |
| | 11 | Mokhovoe Bog | 52.52 | 86.42 | 283 | Blyakharchuk, 2022 |
| | 12 | Kuatang Mire | 51.81 | 87.32 | 650 | Blyakharchuk et al., 2024 |
| D | 13 | Dzhangyskol Lake | 50.18 | 87.73 | 1800 | Blyakharchuk et al., 2008 |
| | 14 | Uzunkol Lake | 50.48 | 87.1 | 1985 | Blyakharchuk et al., 2004 |
| | 15 | Kendegelukol Lake | 50.50 | 87.63 | 2050 | Blyakharchuk et al., 2004 |
| E | 16 | Tashkol Lake | 50.45 | 87.67 | 2150 | Blyakharchuk et al., 2004 |
| | 17 | Akkol Lake | 50.25 | 89.62 | 2204 | Blyakharchuk et al., 2007 |
| | 18 | Grusha Lake | 50.38 | 89.42 | 2413 | Blyakharchuk et al., 2007 |
| F | 19 | Buibinskoye Mire | 52.84 | 93.52 | 1377 | Blyakharchuk et al., 2022 |
| | 20 | Bezrybnoye Mire | 52.81 | 93.50 | 1395 | Blyakharchuk et al., 2022 |
| | 21 | Lugovoe Peat | 52.85 | 93.35 | 1299 | Blyakharchuk et al., 2013 |
| G | 22 | Olgi Lake(OL3) | 48.32 | 98.01 | 2012 | Unkelbach et al., 2021 |
| | 23 | Shireet Naiman Nuur | 46.53 | 101.82 | 2429 | Barhoumi et al., 2024 |
| | 24 | Uggi Nuur | 47.77 | 102.78 | 1330 | Wang et al., 2011 |

https://doi.org/10.5194/egusphere-2025-1991
Preprint. Discussion started: 26 May 2025


**Table 2** Correlation between the independent variables represented by pollen percentages (*Betula*, *Larix*, *Picea*, *Pinus sibirica*, *Pinus sylvestris* and primary forest cover (i.e., the summed percentage values of *Betula*, *Larix*, *Picea* and *Pinus*)) and the dependent variable (biomass burning; charcoal influx). The significance of each parameter is given by p values where ***p < 0.001; **p < 0.01; *p < 0.05.

| Site Name | Independent variable | edf | ref.df | F value | p-value | Deviance explained |
|---|---|---|---|---|---|---|
| Achit Nuur | *Abies* | - | - | - | - | - |
| | *Betula* | 2.75 | 3.47 | 3.40 | 0.02* | 21% |
| | *Larix* | 3.51 | 4.21 | 8.72 | 0.00*** | 41.9% |
| | *Picea* | 1 | 1 | 11.36 | 0.001** | 19.2% |
| | *Pinus sibirica* | 2.73 | 3.41 | 5.70 | 0.001** | 34.5% |
| | *Pinus sylvestris* | - | - | - | - | - |
| | Primary cover | 2.92 | 3.69 | 8.02 | 0.00*** | 41.5% |
| Tolbo Lake | *Abies* | - | - | - | - | - |
| | *Betula* | 6.96 | 8.01 | 1.76 | 0.09 | 7.04% |
| | *Larix* | 1.03 | 1.07 | 0.03 | 0.95 | 0.03% |
| | *Picea* | 2.97 | 3.75 | 4.47 | 0.002** | 8.11% |
| | *Pinus sibirica* | 2.68 | 3.39 | 9.55 | 0.00*** | 13.3% |
| | *Pinus sylvestris* | - | - | - | - | - |
| | Primary cover | 2.98 | 3.75 | 8.96 | 0.00*** | 14.3% |
| Alahake Lake | *Abies* | 1 | 1 | 0.57 | 0.45 | 1.1% |
| | *Betula* | 1 | 1 | 4.19 | 0.04* | 5.2% |
| | *Larix* | 6.85 | 7.94 | 1.42 | 0.19 | 11.6% |
| | *Picea* | 3.84 | 4.77 | 1.96 | 0.09 | 10% |
| | *Pinus sibirica* | 5.59 | 6.77 | 1.85 | 0.09 | 13% |
| | *Pinus sylvestris* | - | - | - | - | - |
| | Primary cover | 2.17 | 2.77 | 1.24 | 0.26 | 5.07% |
| Kuchuk Lake | *Abies* | 1.21 | 1.40 | 3.80 | 0.03* | 9.81% |
| | *Betula* | 1.38 | 1.67 | 16.18 | 0.00*** | 25.2% |
| | *Larix* | 1.11 | 1.21 | 0.01 | 0.98 | 0.19% |
| | *Picea* | 1.16 | 1.30 | 1.31 | 0.30 | 2.29% |
| | *Pinus sibirica* | 5.84 | 6.89 | 1.06 | 0.39 | 9.51% |
| | *Pinus sylvestris* | 6.54 | 7.64 | 2.61 | 0.01* | 25.5% |
| | Primary cover | 3.59 | 4.47 | 1.22 | 0.28 | 11% |
| Rybnaya Mire | *Abies* | 5.28 | 6.31 | 1.99 | 0.07 | 11.7% |
| | *Betula* | 4.90 | 6.00 | 3.32 | 0.004** | 18.4% |
| | *Larix* | 7.07 | 8.11 | 1.95 | 0.07 | 20.6% |
| | *Picea* | 8.15 | 8.79 | 14.1 | 0.00*** | 44.5% |
| | *Pinus sibirica* | 6.74 | 7.86 | 1.68 | 0.12 | 16.6% |
| | *Pinus sylvestris* | 2.03 | 2.54 | 1.06 | 0.35 | 4% |
| | Primary cover | 7.00 | 8.10 | 3.06 | 0.003** | 16.2% |

https://doi.org/10.5194/egusphere-2025-1991
Preprint. Discussion started: 26 May 2025


| | | | | | | |
|---|---|---|---|---|---|---|
| Plotnikovo Mire | *Abies* | 3.12 | 3.88 | 0.70 | 0.55 | 16.7% |
| | *Betula* | 2.69 | 3.36 | 1.40 | 0.26 | 19.6% |
| | *Larix* | 1 | 1 | 4.09 | 0.06 | 20.1% |
| | *Picea* | 2.12 | 2.65 | 1.54 | 0.26 | 15.1% |
| | *Pinus sibirica* | 1.68 | 2.11 | 0.41 | 0.7 | 4.85% |
| | *Pinus sylvestris* | 2.01 | 2.53 | 1.50 | 0.23 | 14.7% |
| | Primary cover | 4.43 | 5.21 | 4.07 | 0.004** | 39.7% |
| Schuchye Lake | *Abies* | 4.78 | 5.85 | 5.39 | 0.00*** | 37.4% |
| | *Betula* | 1 | 1 | 5.29 | 0.03* | 10.8% |
| | *Larix* | 1 | 1 | 63.71 | 0.00*** | 45.4% |
| | *Picea* | 2.19 | 2.71 | 3.77 | 0.02* | 17.5% |
| | *Pinus sibirica* | 1 | 1 | 27.6 | 0.00*** | 30.8% |
| | *Pinus sylvestris* | 3.15 | 3.90 | 3.31 | 0.02* | 21.2% |
| | Primary cover | 2.10 | 2.52 | 7.91 | 0.00*** | 24.7% |
| Ulukh–Chayakh Mire | *Abies* | 6.38 | 7.52 | 1.60 | 0.18 | 29.4% |
| | *Betula* | 1 | 1 | 6.44 | 0.01* | 13.4% |
| | *Larix* | 2.54 | 3.16 | 2.46 | 0.07 | 17.5% |
| | *Picea* | 2.45 | 3.12 | 1.46 | 0.23 | 16.7% |
| | *Pinus sibirica* | 1 | 1 | 0.66 | 0.42 | 1.82% |
| | *Pinus sylvestris* | 1 | 1 | 4.43 | 0.04* | 10.3% |
| | Primary cover | 4.26 | 5.08 | 1.46 | 0.22 | 16.9% |
| Chudnoye Lake | *Abies* | 1.75 | 2.17 | 2.09 | 0.14 | 8.52% |
| | *Betula* | 1.23 | 1.42 | 10.54 | 0.001** | 23.5% |
| | *Larix* | 2.06 | 2.57 | 3.84 | 0.03* | 14.7% |
| | *Picea* | 1.99 | 2.44 | 11.76 | 0.00*** | 30.3% |
| | *Pinus sibirica* | 4.33 | 5.25 | 3.38 | 0.01* | 26.6% |
| | *Pinus sylvestris* | 1 | 1 | 6.59 | 0.01* | 11.6% |
| | Primary cover | 1 | 1 | 1.97 | 0.17 | 3.5% |
| Tundra Mire | *Abies* | 2.16 | 2.75 | 0.78 | 0.57 | 3.83% |
| | *Betula* | 1 | 1 | 3.27 | 0.07 | 4.44% |
| | *Larix* | 6.41 | 7.35 | 4.32 | 0.00*** | 22.7% |
| | *Picea* | 1 | 1 | 0.09 | 0.77 | 0.13% |
| | *Pinus sibirica* | 2.39 | 2.99 | 0.83 | 0.46 | 4.66% |
| | *Pinus sylvestris* | 3.03 | 3.78 | 0.79 | 0.49 | 5.83% |
| | Primary cover | 1 | 1 | 2.79 | 0.10 | 3.53% |
| Mokhove Bog | *Abies* | 1.83 | 2.31 | 1.12 | 0.38 | 3.65% |
| | *Betula* | 6.81 | 7.88 | 2.07 | 0.05 | 17.2% |
| | *Larix* | 1.09 | 1.17 | 0.24 | 0.63 | 0.59% |
| | *Picea* | 2.59 | 3.22 | 3.54 | 0.02* | 11.9% |
| | *Pinus sibirica* | 1 | 1 | 0.00 | 0.96 | 0.003% |
| | *Pinus sylvestris* | 4.46 | 5.49 | 1.78 | 0.11 | 13% |
| | Primary cover | 5.04 | 6.19 | 0.91 | 0.48 | 10.3% |
| Kuatang | *Abies* | 2.45 | 3.14 | 2.78 | 0.04* | 13.8% |

https://doi.org/10.5194/egusphere-2025-1991
Preprint. Discussion started: 26 May 2025


| | | | | | | |
|---|---|---|---|---|---|---|
| Mire | *Betula* | 1 | 1 | 29.13 | 0.00*** | 24.5% |
| | *Larix* | 1 | 1.00 | 0.06 | 0.81 | 0.08% |
| | *Picea* | 6.72 | 7.79 | 1.19 | 0.31 | 13.4% |
| | *Pinus sibirica* | 1.43 | 1.74 | 2.92 | 0.05* | 6.90% |
| | *Pinus sylvestris* | 1 | 1 | 5.83 | 0.02* | 6.51% |
| | Primary cover | 1 | 1 | 9.24 | 0.003** | 10.9% |
| Dzhangyskol Lake | *Abies* | 3.64 | 4.53 | 0.45 | 0.79 | 16.9% |
| | *Betula* | 1.79 | 2.23 | 0.37 | 0.77 | 7.12% |
| | *Larix* | 1 | 1 | 0.05 | 0.83 | 0.33% |
| | *Picea* | 3.92 | 4.80 | 0.82 | 0.51 | 24.8% |
| | *Pinus sibirica* | 1.70 | 2.12 | 0.35 | 0.73 | 7.06% |
| | *Pinus sylvestris* | 3.05 | 3.75 | 1.22 | 0.29 | 22.8% |
| | Primary cover | 2.39 | 3.04 | 0.67 | 0.58 | 15.6% |
| Uzunkol Lake | *Abies* | 1 | 1 | 5.329 | 0.02* | 7.04% |
| | *Betula* | 4.92 | 5.99 | 3.22 | 0.01** | 29.4% |
| | *Larix* | 1 | 1 | 14.38 | 0.00*** | 22.1% |
| | *Picea* | 5.99 | 7.12 | 5.03 | 0.00*** | 40.1% |
| | *Pinus sibirica* | 2.04 | 2.57 | 1.99 | 0.14 | 14.7% |
| | *Pinus sylvestris* | 4.79 | 5.81 | 2.85 | 0.02* | 29.3% |
| | Primary cover | 2.17 | 2.69 | 1.39 | 0.27 | 14.2% |
| Kendegelukol Lake | *Abies* | 4.93 | 5.97 | 2.63 | 0.04* | 41.4% |
| | *Betula* | 5.87 | 7.04 | 2.78 | 0.02* | 49.4% |
| | *Larix* | 1 | 1 | 3.11 | 0.09 | 9.63% |
| | *Picea* | 2.99 | 3.73 | 2.19 | 0.08 | 29.4% |
| | *Pinus sibirica* | 2.25 | 2.78 | 2.26 | 0.09 | 28.9% |
| | *Pinus sylvestris* | 1 | 1 | 18.48 | 0.00*** | 40% |
| | Primary cover | 1.57 | 1.91 | 3.58 | 0.06 | 26.9% |
| Tashkol Lake | *Abies* | 1 | 1 | 0.02 | 0.90 | 0.09% |
| | *Betula* | 1 | 1 | 0.08 | 0.79 | 0.36% |
| | *Larix* | 1.56 | 1.92 | 0.20 | 0.82 | 3.52% |
| | *Picea* | 6.69 | 7.81 | 2.35 | 0.04* | 40.7% |
| | *Pinus sibirica* | 1 | 1 | 0.004 | 0.95 | 0.02% |
| | *Pinus sylvestris* | 1 | 1 | 0.02 | 0.89 | 0.09% |
| | Primary cover | 3.00 | 3.75 | 0.90 | 0.48 | 17% |
| Akkol Lake | *Abies* | 1.76 | 2.11 | 0.79 | 0.43 | 4.83% |
| | *Betula* | 1 | 1 | 0.96 | 0.33 | 1.76% |
| | *Larix* | 6.53 | 7.59 | 1.94 | 0.08 | 30.4% |
| | *Picea* | 2.41 | 3.03 | 6.77 | 0.00*** | 31.6% |
| | *Pinus sibirica* | 4.35 | 5.41 | 1.90 | 0.1 | 23% |
| | *Pinus sylvestris* | 1 | 1 | 10.12 | 0.002** | 18.9% |
| | Primary cover | 8.47 | 8.92 | 5.49 | 0.00*** | 55.1% |
| Grusha | *Abies* | 1 | 1 | 0.62 | 0.44 | 2.75% |

https://doi.org/10.5194/egusphere-2025-1991
Preprint. Discussion started: 26 May 2025


| | | | | | | |
|---|---|---|---|---|---|---|
| Lake | *Betula* | 1 | 1 | 0.88 | 0.36 | 3.93% |
| | *Larix* | 3.81 | 4.58 | 3.44 | 0.02* | 49.3% |
| | *Picea* | 2.18 | 2.71 | 3.30 | 0.05* | 35.80% |
| | *Pinus sibirica* | 1 | 1 | 0.60 | 0.45 | 2.67% |
| | *Pinus sylvestris* | 1.39 | 1.66 | 0.19 | 0.76 | 4.67% |
| | Primary cover | 2.55 | 3.18 | 12.7 | 0.00*** | 71.1% |
| Bezrybnoe Mire | *Abies* | 1.15 | 1.29 | 0.31 | 0.75 | 1.16% |
| | *Betula* | 1.74 | 2.20 | 1.63 | 0.22 | 8.85% |
| | *Larix* | 2.58 | 3.14 | 0.32 | 0.79 | 4.76% |
| | *Picea* | 1 | 1 | 2.13 | 0.15 | 4.49% |
| | *Pinus sibirica* | 1.37 | 1.66 | 0.39 | 0.75 | 2.18% |
| | *Pinus sylvestris* | 6.47 | 7.53 | 1.69 | 0.13 | 28.1% |
| | Primary cover | 1 | 1 | 0.01 | 0.93 | 0.02% |
| Buibinskoye Mire | *Abies* | 2.71 | 3.39 | 4.85 | 0.004** | 29.6% |
| | *Betula* | 2.11 | 2.69 | 2.29 | 0.10 | 17.4% |
| | *Larix* | 1 | 1 | 1.16 | 0.29 | 2.83% |
| | *Picea* | 1.52 | 1.87 | 0.71 | 0.40 | 4.85% |
| | *Pinus sibirica* | 2.02 | 2.57 | 2.70 | 0.05 | 17.4% |
| | *Pinus sylvestris* | 1 | 1 | 3.78 | 0.06 | 7.42% |
| | Primary cover | 3.61 | 4.42 | 2.47 | 0.06 | 22.6% |
| Lugovoe Mire | *Abies* | 1 | 1 | 6.32 | 0.02* | 15.3% |
| | *Betula* | 1 | 1 | 0.23 | 0.64 | 0.79% |
| | *Larix* | 5.00 | 5.91 | 3.89 | 0.01** | 43.5% |
| | *Picea* | 4.00 | 4.95 | 2.41 | 0.07 | 35.8% |
| | *Pinus sibirica* | 3.43 | 4.28 | 2.20 | 0.09 | 31% |
| | *Pinus sylvestris* | 8.81 | 8.98 | 3.21 | 0.01* | 60.5% |
| | Primary cover | 1.14 | 1.27 | 0.20 | 0.67 | 2.29% |
| Olgi Lake | *Abies* | - | - | - | - | - |
| | *Betula* | 4.89 | 5.96 | 2.91 | 0.02* | 34.5% |
| | *Larix* | 4.32 | 5.29 | 2.68 | 0.03* | 35.6% |
| | *Picea* | 3.8 | 4.65 | 4.20 | 0.003** | 35.7% |
| | *Pinus sibirica* | 8.62 | 8.89 | 45.23 | 0.00*** | 27.9% |
| | *Pinus sylvestris* | - | - | - | - | - |
| | Primary cover | 1.74 | 2.21 | 7.46 | 0.00*** | 33.3% |
| Shireet Naiman Nuur | *Abies* | - | - | - | - | - |
| | *Betula* | 2.57 | 3.211 | 3.82 | 0.01* | 20.7% |
| | *Larix* | 1 | 1 | 1.59 | 0.21 | 2.83% |
| | *Picea* | 1 | 1 | 6.55 | 0.01* | 9.70% |
| | *Pinus sibirica* | 3.98 | 4.91 | 4.02 | 0.003** | 27.5% |
| | *Pinus sylvestris* | 1 | 1 | 7.99 | 0.01** | 12% |
| | Primary cover | 4.01 | 4.96 | 6.38 | 0.00*** | 37.4% |
| Uggi Nuur | *Abies* | - | - | - | - | - |
| | *Betula* | 6.49 | 7.59 | 2.02 | 0.06 | 8.65% |

https://doi.org/10.5194/egusphere-2025-1991
Preprint. Discussion started: 26 May 2025


| | | | | | | |
|---|---|---|---|---|---|---|
| | *Larix* | 6.48 | 0.06 | 104.4 | 0.00*** | 12.2% |
| | *Picea* | 1 | 1 | 0.18 | 0.67 | 0.1% |
| | *Pinus sibirica* | 8.55 | 8.94 | 6.19 | 0.00*** | 19.4% |
| | *Pinus sylvestris* | - | - | - | - | - |
| | Primary cover | 8.07 | 8.76 | 5.72 | 0.00*** | 18.4% |